Astron. Astrophys. 344, 188–198 (1999)

ASTRONOMY AND ASTROPHYSICS

Light perturbation from stellar nonradial oscillations: an application to solar oscillations

T. Toutain, G. Berthomieu, and J. Provost

Observatoire de Nice, B.P. 4229, F-06304 Nice Cedex 4, France

Received 17 July 1998 / Accepted 23 December 1998

Abstract. We derive analytical expressions for the emerging intensity and flux perturbations due to stellar nonradial oscillations taking into account the sphericity of the emitting layers. These expressions are derived using both the Eulerian and Lagrangian formulations. We show, analytically and numerically, that these formulations are equivalent and that they lead, in the limit of a plane-parallel atmosphere, to analytical expressions derived in previous works. As an example, we compute for a grey atmosphere intensity perturbations for low-degree solar oscillations and show that some p and g modes can produce large variations of intensity on the very limb of the solar disk. We also compute the corresponding flux perturbations showing that differences between spherical and plane-parallel computations for modes below 4 mHz do not exceed 15 percents, the better agreement being for low frequencies.

Key words: Sun: oscillations – stars: oscillations – stars: atmospheres

1. Introduction

Detection and identification of low-degree solar p and g modes of low order are useful if we want to go further in the understanding of the physics and the rotation of the core of the Sun. Unfortunately, even with the longest helioseismologic data sets no g modes were, up to now, unambiguously detected neither for velocity measurements nor with intensity measurements. Theoretical supports are therefore needed to help the search of g modes. One of these supports is the estimation of theoretical g-mode amplitudes for intensity measurements. These theoretical amplitudes allow us to build theoretical g-mode power spectra to be compared to observational ones. The pioneering work in this domain is the paper of Dziembowski (1977). Assuming that the emerging intensity perturbation due to an oscillation is known, Dziembowski derives the corresponding perturbation of flux and the effect of surface distortion on it. Then Buta & Smith (1979) give an expression for the emerging intensity perturbation assuming adiabatic oscillations and modeling the stellar atmosphere as a blackbody surface. A step forward is accomplished in the paper by Berthomieu & Provost (1990) where the thickness of the atmosphere is taken into account and in the papers of Toutain & Gouttebroze (1993) and Staude et al. (1994) where, in the case of the Sun, the radiative transfer in the photosphere is taken into account as well as the opacity perturbation due to nonradial oscillations. Nevertheless, these works still suffer three approximations:

- a plane-parallel atmosphere is assumed for computing the emerging intensity,
- nonadiabatic coupling between g modes and convection is neglected,
- g-mode amplitudes are computed assuming energy equipartition.

Improving the last two approximations is difficult. For the coupling see e.g. the works of Gough (1977), Gonczi & Osaki (1980) and more recently the work of Balmforth (1992). For the g-mode energy see (Andersen 1996) who simulates excitation of g modes by the convective overshooting at the base of the solar convection zone and (Kumar et al. 1996) who assume the fluctuating Reynolds stress to be the source of g-mode excitation. Up to now, the mechanisms exciting g modes are unknown and the distribution of energy in the modes as a function of their frequency and their degree is also unknown.

In this paper we derive analytical expressions of the amplitudes of nonradial oscillations for full-disc intensity observations in the visible continuum, taking into account the sphericity of the photosphere. As an application we compute these amplitudes for low-degree solar p and g modes.

In the next section we verify analytically that Eulerian and Lagrangian formulations can equivalently be used to derive the amplitude of the intensity perturbation due to a nonradial oscillation. In the third section we derive the amplitude of the flux perturbation in the general spherical case. For the plane-parallel case, we show that with some constraints we are able to derive the flux perturbation with its geometrical terms as given by Toutain & Gouttebroze (1993). In the fourth section we compute intensity and flux perturbations for low-degree solar oscillations and compare flux perturbations of the spherical case to flux perturbations of the plane-parallel case. We also compare the efficiency for numerical purpose of Eulerian and Lagrangian formulations.

Send offprint requests to: T. Toutain

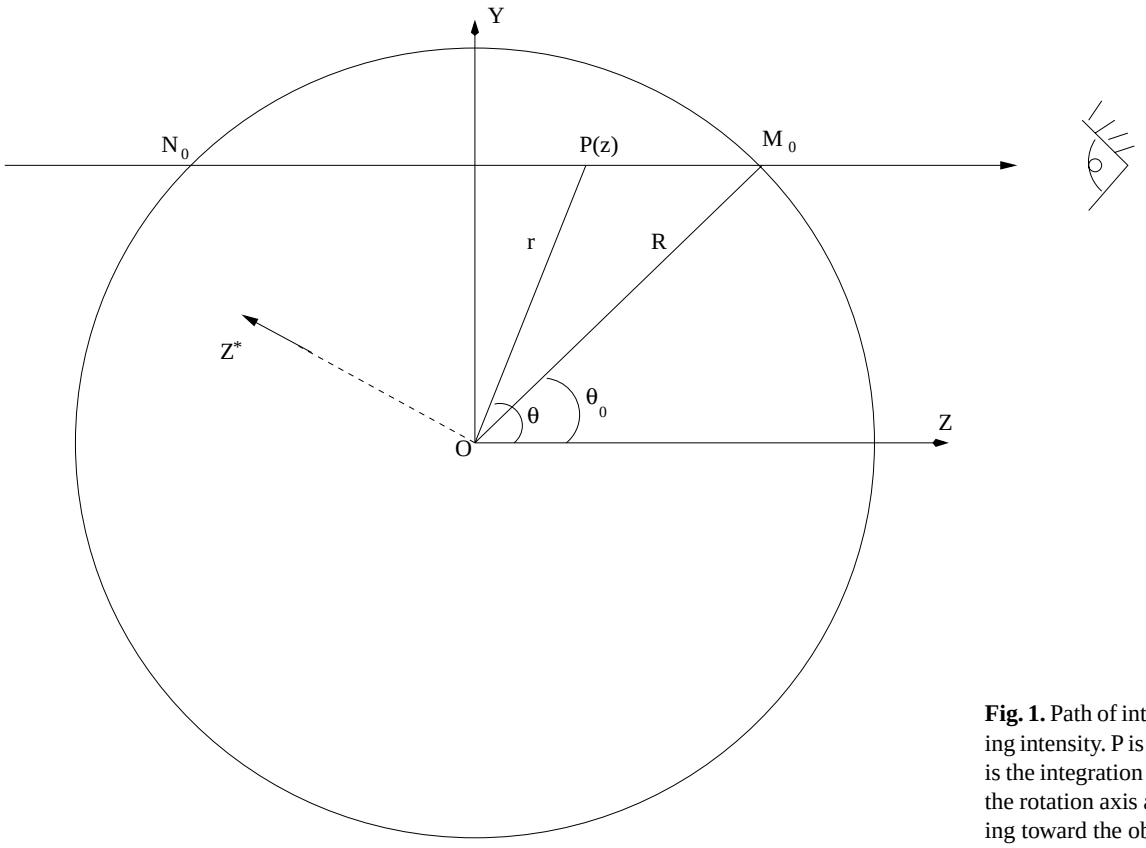

Fig. 1. Path of integration for the emerging intensity. P is the running point and z is the integration variable, the Z*-axis is the rotation axis and the Z-axis is pointing toward the observer

2. From Euler to Lagrange formulation

In order to derive analytical expressions for the perturbation of stellar light in the visible continuum due to a nonradial oscillation we need to derive the perturbation of the emerging intensity on the visible hemisphere. Let us first define for equilibrium (no oscillation) the quantities of the problem and the corresponding emerging intensity. For a sufficiently slowly rotating star, like the Sun, we can neglect the deformation due to rotation and assume a spherical shape at equilibrium. We therefore assume the star to be centered at point O with a radius R and having its rotation axis along the Z*-axis (see Fig. 1).

We define (0, X*, Y*, Z*) to be the main frame of the star and (r, θ^*, ϕ^*)the corresponding spherical coordinates. Moreover, assuming a Z-axis pointing toward an observer we consider an other frame (O, X, Y, Z) called the observer frame and (r, θ, ϕ) the corresponding spherical coordinates. Therefore the position of each point M_0 on the visible surface will be defined in the observer frame by the usual spherical coordinates (R, θ_0, ϕ_0). We will also frequently use the quantity μ_0 which is the cosine of θ_0. The observer is assumed far enough from the star (on a scale of R) such as the line of sight at M_0 is parallel to the Z-axis. We denote also N_0 as the point on the nonvisible surface symmetric to M_0. The coordinates of M_0 and N_0 on the Z-axis will be denoted Z_0 and -Z_0 respectively.

At equilibrium, the monochromatic intensity $I_\nu^{(0)}$ at light frequency ν emerging from M_0 towards the observer will be obtained integrating the contribution of each element of fluid between N_0 and M_0 along the line of sight, assuming no radiation is entering the star. Since the line of sight at M_0 is parallel to the Z-axis we use the integration variable z and write (e.g. Chandrasekhar 1960):

$$I_\nu^{(0)}(\mu_0, \phi_0) = \int_{-Z_0}^{Z_0} \epsilon_\nu(z) e^{-\eta_\nu} \, \mathrm{d}z \tag{1}$$

where

$$\eta_\nu(z) = \int_z^{Z_0} \alpha_\nu(z) \, \mathrm{d}z \tag{2}$$

$$\alpha_\nu(z) = \kappa_\nu \rho \tag{3}$$

and

$$\epsilon_\nu(z) = \alpha_\nu S_\nu \tag{4}$$

$\eta_\nu(z)$ is the monochromatic optical thickness along the line of sight. ϵ_ν, α_ν are the monochromatic volume emission coefficient and volume absorption coefficient, respectively. Note that because of the spherical symmetry of the star $I_\nu^{(0)}$ does not depend on ϕ_0.

We assume now that the star is oscillating around its equilibrium position, and to avoid tackling with nonlinear physics, we consider only small perturbations of the equilibrium state. There are two different ways of describing the perturbation of the medium. The first one is the Eulerian formulation. In this case, we are interested in the changes of temperature, pressure, density... at a given point of space as a function of time. Thus

for example T'($\boldsymbol{r}$,t) corresponds to the temperature perturbation at position $\boldsymbol{r}$ and time t. The second one is the Lagrangian formulation for which we are interested in the same changes but in a given fluid element as a function of time. Thus for example δT(A($\boldsymbol{r}$),t) corresponds to the temperature perturbation of the fluid element A($\boldsymbol{r}$) at time t. In this paper the symbol ' will always indicate the Eulerian perturbation of a quantity whereas δ will indicate the corresponding Lagrangian perturbation. These formulations are equivalent and to switch from one to the other we use the formula, written here as an example for temperature,

$$\delta T(A(\boldsymbol{r}),t) = T'(\boldsymbol{r},t) + \delta r \frac{dT}{dr} \tag{5}$$

where δr is the radial displacement of matter. Because we use the variable z rather than r, we rewrite Eq. (5) as:

$$\delta T(A(z),t) = T'(z,t) + \frac{\delta r}{\mu}\frac{dT}{dz} \tag{6}$$

where

$$dz = \frac{dr}{\mu} \tag{7}$$

has been used (μ is the cosine of θ). Following now a normal mode decomposition technique we write each perturbation, here as an example for the radial displacement, as

$$\delta r = \xi_r(r).Y_{lm}(\theta^*,\phi^*).e^{i\omega t} \tag{8}$$

where we have introduced the temporal and the angular dependence of the eigenfunctions. The angles are labeled with an asterisk indicating that they are referenced to the main frame of the star. Y_{lm} the usual spherical harmonic function is used to take advantage of the spherical symmetry of the star.

The above described perturbations of temperature, density and pressure in the photosphere, as well as the displacement of the matter produce a perturbation of the emission and absorption coefficients as well as the optical thickness. Consequently these perturbations of the medium induce also a perturbation of the visible continuum intensity emerging in the observer direction, continuum which is mainly formed in the photosphere. We define this perturbation as the following

$$\Delta I_\nu(\mu_0,\phi_0,t) \equiv I_\nu(\mu_0,\phi_0,t) - I_\nu^{(0)}(\mu_0) \tag{9}$$

Using a stellar model it is possible to compute $I_\nu^{(0)}(\mu_0)$ for each μ_0. The problem is rather how can we compute the other term $I_\nu(\mu_0,\phi_0,t)$? To go further, we therefore need to give a theoretical expression for the perturbation of emerging intensity as a function of the displacement of the fluid and the perturbation of the emission and absorption coefficients. Arises now the question "Shall we use an Eulerian or a Lagrangian formulation to describe the problem?". To answer this question we have to answer first the related question "What is the meaning of an intensity perturbation with both formulations?". Because of the definition of the emerging intensity, see Eq. (1), only the fluid elements crossing the line of sight contribute to the intensity observed. Therefore the Eulerian formulation is certainly more appropriate to compute the perturbation of emerging intensity, because it is not necessary to know which fluid elements are on the line of sight at each time as it is with Lagrangian formulation. Thus, in this section we start with deriving the perturbation of emerging intensity using the Eulerian approach. Nevertheless, though the Lagrangian formulation is less "natural" than the Eulerian one for this problem, it is very convenient for numerical purposes as shown in Sect. 4. This is why, in the present section, we give also a Lagrangian expression for the perturbation of emerging intensity and demonstrate the equivalence of both formulations.

2.1. Derivation of the intensity perturbation using the Eulerian formulation

When the star is oscillating its surface is slightly distorted and the matter contributing to the emerging intensity is no longer bounded in M_0 and N_0 but rather in M(t) and N(t) which are the intersection between the line of sight and the distorted surface and which are therefore a function of time, see Fig. 2. We denote:

$$\Delta Z(M_0) = Z(M) - Z_0 \tag{10}$$

and

$$\Delta Z(N_0) = Z(N) + Z_0 \tag{11}$$

The emerging intensity from the perturbed star is:

$$\begin{aligned} I_\nu(\mu_0,\phi_0,t) \;=\; & \int_{Z(N)}^{Z(M)} (\epsilon_\nu + \epsilon'_\nu). \\ & exp\left(-\int_z^{Z(M)} (\eta_\nu + \eta'_\nu)\mathrm{d}z\right)\,\mathrm{d}z \end{aligned} \tag{12}$$

Using Eqs. 1 and 12 in Eq. (9) and keeping only first order terms, the perturbation of emerging intensity reads:

$$\begin{aligned} \Delta I(\mu_0,\phi_0,t) \;=\; & I_\nu^a(\mu_0,\phi_0,t) + I_\nu^b(\mu_0,\phi_0,t) \\ & + I_\nu^c(\mu_0,\phi_0,t) \end{aligned} \tag{13}$$

To avoid heavy notations we will ignore here below the time dependence and the frequency dependence of all the quantities. The first term:

$$I^a(\mu_0,\phi_0) = \int_{-Z_0}^{Z_0} \left[\frac{\epsilon'}{\epsilon} - \int_z^{Z_0} \alpha' \mathrm{d}z\right] \epsilon(z) e^{-\eta}\,\mathrm{d}z \tag{14}$$

comes from the Eulerian perturbations of the integrand in Eq. (12), whereas the second term

$$I^b(\mu_0,\phi_0) = -\alpha(Z_0)\Delta Z(M_0)\; I^{(0)}(\mu_0) \tag{15}$$

comes from the perturbation of the upper boundary of the optical thickness in Eq. (12) and the third term

$$\begin{aligned} I^c(\mu_0,\phi_0) \;=\; & \epsilon(Z_0)\;\Delta Z(M_0) - \\ & \epsilon(-Z_0)\;\Delta Z(N_0)\; exp(-\int_{-Z_0}^{Z_0} \eta(z)\,\mathrm{d}z) \end{aligned} \tag{16}$$

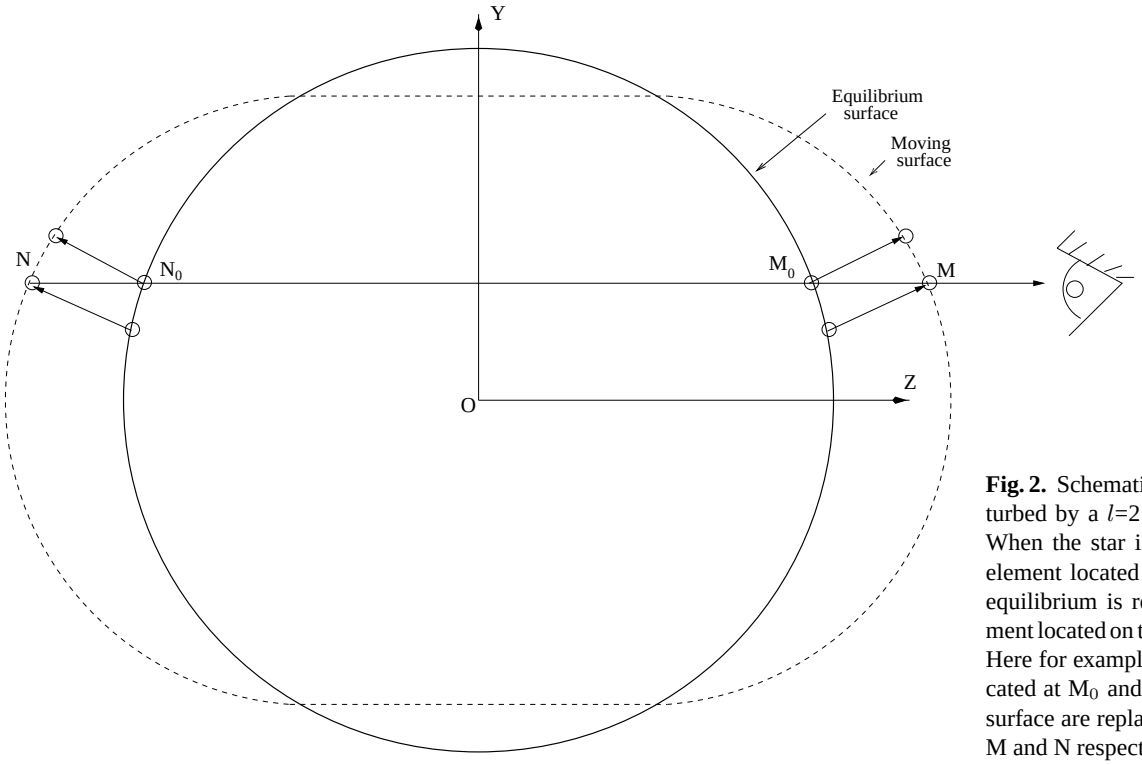

Fig. 2. Schematic shape of a star perturbed by a *l*=2 g mode (dashed line). When the star is perturbed, each fluid element located on the line of sight at equilibrium is replaced by a fluid element located on the same spherical shell. Here for example the fluid elements located at M_0 and N_0 on the equilibrium surface are replaced by those located at M and N respectively.

comes from the perturbation of the boundaries of the integral in Eq. (12). From a physical point of view, I^a is due to the changes of the local properties of the medium between M_0 and N_0, I^b is the contribution of transparency changes to the perturbed emerging intensity because of the surface distortion at point M_0, while I^c corresponds to changes of the emerging intensity due to the displacements of matter around M_0 and N_0. Note that in the paper by Gouttebroze & Toutain (1994) I^b and I^c were not taken into account because the authors assumed α and ϵ to be vanishing at the surface. From a computational point of view, the last points of stellar models have nonzero values for α and ϵ making I^b and I^c not always negligible compared to I^a, especially close to the limb. The Eulerian perturbation of emerging intensity given by Eq. (13) is therefore a sum of three terms which seem easily computable. Unfortunately, we find out numerically that the emission and the absorption contributions to I^a cancel each other almost exactly and the remainder of this cancellation is the quantity we are looking at. Therefore the computation of the emerging intensity perturbation is somehow difficult as shown in Sect. 4. One way to avoid this problem is to do the cancellation analytically taking advantage of the Lagrangian description.

2.2. Derivation of the intensity perturbation using the Lagrangian formulation

We introduce in Eq. (14) Eq. (6) which is the usual relation between Eulerian and Lagrangian perturbation and separate the Lagrangian terms from the advection terms, doing so we get:

$$I^a(\mu_0,\phi_0) = I^d(\mu_0,\phi_0) + I^e(\mu_0,\phi_0) \tag{17}$$

where

$$I^d(\mu_0,\phi_0) = \int_{-Z_0}^{Z_0} \left[\frac{\delta\epsilon}{\epsilon} - \int_z^{Z_0} \delta\alpha \mathrm{d}z\right] \epsilon(z) e^{-\eta}\,\mathrm{d}z \tag{18}$$

and

$$I^e(\mu_0,\phi_0) = \int_{-Z_0}^{Z_0} \left[-\frac{d\epsilon}{\epsilon dz}\frac{\delta r}{\mu} + \int_z^{Z_0} \frac{d\alpha}{dz}\frac{\delta r}{\mu}\mathrm{d}z\right] \times\epsilon(z)e^{-\eta}\,\mathrm{d}z \tag{19}$$

It turns out that the advection terms of Eq. (19) are larger than the Lagrangian terms of Eq. (18) by several orders of magnitude. But I^e is of the same order of magnitude as I^d because the advection terms of emission compensate almost exactly those of absorption. The problem of cancellation described in the previous section comes therefore from the advection terms which are implicitly contained in the Eulerian perturbation. This fact explains why computing I^a accurately is not so easy. On the other hand computing I^d accurately is not a problem. We can now proceed analytically to the cancellation of the advection terms by integrating by part I^e. Doing so we face a new problem which is that the new integral is diverging for points satisfying μ=0 because of the term $1/\mu$ appearing in I^e. Nevertheless these points located in the plane Z=0 generally do not contribute to the emerging intensity because the opacity increases very rapidly inwards along the line of sight. Only close to the limb of the star the other hemisphere contributes significantly to the emerging intensity and these points have to be taken into acount. For example, in the case of the Sun these points contribute only when $0 \leq \mu \leq 0.03$ that is to say the domain where Eq. (17) is not applicable corresponds to the very limb. Of course for stars having

an extended atmosphere this domain can be a significant part of the disc.

Assuming the opacity to increase rapidly along the line of sight we neglect the contribution of matter beyond an arbitrary point Q both in Eqs. (18) and (19) and integrate by part the integral of Eq. (19) obtaining:

$$I^e(\mu_0,\phi_0) = \int_{Z(Q)}^{Z_0} \left[\frac{d(\delta r/\mu)}{\epsilon dz} - \int_z^{Z_0} \alpha \frac{d(\delta r/\mu)}{dz} \mathrm{d}z\right] \epsilon(z) e^{-\eta} \mathrm{d}z - I^b(\mu_0,\phi_0) - I^c_{QM_0}(\mu_0,\phi_0) \quad (20)$$

$I^c_{QM_0}$ is the same as in Eq. (16) but with Z(Q) instead of -Z_0. Inserting now Eqs. (18) and (20) in Eq. (13) where Z(Q) instead of -Z_0 is used as lower boundary we get the Lagrangian expression for the perturbation of emerging intensity:

$$\Delta I(\mu_0,\phi_0) = \int_{-Z(Q)}^{Z_0} \left[\frac{\delta\epsilon}{\epsilon} + \frac{d(\delta r/\mu)}{\epsilon dz} - \int_z^{Z_0} (\delta\alpha + \alpha \frac{d(\delta r/\mu)}{dz})\, \mathrm{d}z\right] \epsilon(z) e^{-\eta}\, \mathrm{d}z \quad (21)$$

Though the fluid elements contributing to the emerging intensity are changing with time we are still able to write the perturbation of emerging intensity in terms of only Lagrangian quantities. We need therefore to understand the physical meaning of Eq. (21). Looking at Fig. 2 we see that both the fluid elements located at M_0 and N_0 on the surface are replaced on the line of sight when the star oscillates with the fluid elements located at M and N on the perturbed surface. Moreover these fluid elements have the same physical properties than the two previous ones because they come from the same spherical shell at equilibrium. Therefore it is as if the fluid elements have moved from M_0 to M and N_0 to N, respectively. We can imagine replacing the same way each fluid element located at Q_0 between M_0 and N_0 with a fluid element coming from the same spherical shell as Q_0 and located at Q which is the intersection between the line of sight and the perturbed shell. Note that Q is a function of time. Nevertheless, we can see that close to the limb this replacement is impossible because the line of sight and the corresponding perturbed shell are not always intersecting there. This fact explains the problem we faced for the integration by part of I^e. The meaning of Eq. (21) is now obvious: each fluid element on the line of sight is replaced at each time with an other fluid element coming from the same spherical shell, it is as if the original fluid element was moving along the line of sight. The displacement of this pseudo-element is given as:

$$\delta z \equiv z(Q) - z(Q_0) \quad (22)$$

δz is therefore not a real displacement of matter but we can write it as a function of radial and horizontal displacements of a fluid element. Defining $\boldsymbol{r}_Q$ and $\boldsymbol{r}_{Q_0}$ as the vectors giving the equilibrium position of the fluid elements located at Q and Q_0, respectively and $\delta\boldsymbol{r}$ as the displacement vector of the fluid element located at Q which is, to the first order, the same as the displacement vector of the fluid element located at Q_0, we have the vectorial equality

$$\boldsymbol{r}_{Q_0} + \delta\boldsymbol{z} = \boldsymbol{r}_Q + \delta\boldsymbol{r} \quad (23)$$

Taking now the squared norm of Eq. (23) and keeping only the first order terms, we get:

$$\delta z = \frac{\delta r}{\mu} \quad (24)$$

as long as $|\mu| \gg \sqrt{\left|\frac{\delta r}{r}\right|}$. It is interesting to note that δz is, to the first order approximation, independent of the horizontal displacement unless this one is very large compared to the radial displacement. Using Eq. (24) in Eq. (21) we obtain

$$\Delta I(\mu_0,\phi_0) = \int_{-Z(Q)}^{Z_0} \left[\frac{\delta\epsilon}{\epsilon} + \frac{d(\delta z)}{\epsilon dz} - \int_z^{Z_0} (\delta\alpha + \alpha \frac{d(\delta z)}{dz})\, \mathrm{d}z\right] \times \epsilon(z) e^{-\eta}\, \mathrm{d}z \quad (25)$$

where

$$\frac{d\delta z}{dz} = \frac{d\xi_r}{dr} Y_{lm}(\theta^*,\phi^*) + \frac{\xi_r}{r} \frac{1-\mu^2}{\mu} \left(\frac{\partial Y_{lm}(\theta^*,\phi^*)}{\partial\mu} - \frac{Y_{lm}(\theta^*,\phi^*)}{\mu}\right) \quad (26)$$

is obtained using Eqs. (24), (7) and (8). Note that Eq. (25) could have been obtained applying the Lagrangian operator to Eq. (1), the only problem being the meaning of δz which is now clarified.

The equality of Eqs. (13) and (25) demonstrates the equivalence between Eulerian and Lagrangian formulations for the computation of the emerging intensity perturbation, except near the limb as pointed out previously. Before deriving the perturbation of flux, we discuss a special case which is the plane-parallel approximation.

2.3. The plane-parallel approximation

The aim of this section is to give an analytical expression for intensity in the limit-case of the plane-parallel approximation which is relevant for the Sun where the thickness of the photosphere is very small compared to the solar radius. This approximation was used by Berthomieu & Provost (1990) and by Toutain & Gouttebroze (1993) with a Lagrangian formulation. For the sake of comparison we derive the perturbation of intensity using Eq. (25) rather than Eq. (13). As in the previous papers, we use instead of z the natural variable of integration τ, the optical depth:

$$\tau = \int_0^h \alpha\, \mathrm{d}h \quad (27)$$

where h = R - r(z) is the depth relative to the surface. Assuming a plane-parallel geometry we can write that $\mu = \mu_0$ along the Z-axis, then changing z to h in Eqs. (1) and (25), we get

$$I^{//}(\mu_0) = \int_0^{+\infty} S(\tau) e^{-\tau/\mu_0} \frac{\mathrm{d}\tau}{\mu_0} \quad (28)$$

the emerging intensity and

$$\Delta I(\mu_0,\phi_0) = \delta I^{//}(\mu_0,\phi_0) + I^g(\mu_0,\phi_0) \tag{29}$$

the perturbation of emerging intensity, where

$$\begin{aligned}&\delta I^{//}(\mu_0,\phi_0)\\ &= \int_0^{\tau_{max}} \left[\frac{\delta\epsilon}{\epsilon} + \frac{d\xi_r}{dr}Y_{lm} - \int_0^{\tau}(\frac{\delta\alpha}{\alpha} + \frac{d\xi_r}{dr}Y_{lm})\frac{\mathrm{d}\tau}{\mu_0}\right]\\ &\quad S(\tau)e^{-\tau/\mu_0}\,\frac{\mathrm{d}\tau}{\mu_0}\end{aligned} \tag{30}$$

and

$$\begin{aligned}&I^g(\mu_0,\phi_0)\\ &= \int_0^{\tau_{max}} \left[\frac{d\delta z}{dz} - \frac{d\xi_r}{dr}Y_{lm} - \int_0^{\tau}(\frac{d\delta z}{dz} - \frac{d\xi_r}{dr}Y_{lm})\frac{d\tau}{\mu_0}\right]\\ &\quad S(r)e^{-\tau/\mu_0}\,\frac{\mathrm{d}\tau}{\mu_0}\end{aligned} \tag{31}$$

τ_{max} is the optical depth of the point Q where we stop the integration. Introducing Eq. (26) in Eq. (31) and neglecting the variation of ξ_r/r relatively to h we can rewrite

$$\begin{aligned}I^g(\mu_0,\phi_0) \;=\; &\frac{\xi_r}{r}\left[(\mu_0^2-1)\frac{\partial Y_{lm}(\theta_0^*,\phi_0^*)}{\partial\mu_0} + \right.\\ &\left.\frac{(1-\mu_0^2)}{\mu_0}Y_{lm}(\theta_0^*,\phi_0^*)\right]\frac{dI^{//}(\mu_0)}{d\mu_0}\end{aligned} \tag{32}$$

How does Eq. (29) compare to the perturbation of intensity found by Toutain & Gouttebroze (1993)?:

$$\begin{aligned}\Delta I^{//}(\mu_0,\phi_0) \;=\; &\delta I^{//}(\mu_0,\phi_0) + \frac{\xi_r}{r}(\mu_0^2-1)\frac{\partial Y_{lm}(\theta_0^*,\phi_0^*)}{\partial\mu_0}\\ &\frac{dI^{//}(\mu_0)}{d\mu_0}\end{aligned} \tag{33}$$

where the first and second terms on the right side describe the effect on the emerging intensity of thermodynamical changes of the medium and changes of the local normal of the solar surface, respectively. A straight comparison of Eqs. (29) and (33) shows that:

$$\begin{aligned}\Delta I(\mu_0,\phi_0) \;=\; &\Delta I^{//}(\mu_0,\phi_0)\\ &+\frac{(1-\mu_0^2)}{\mu_0}\frac{dI^{//}}{d\mu_0}\frac{\xi_r}{r}Y_{lm}(\theta_0^*,\phi_0^*)\end{aligned} \tag{34}$$

This discrepancy between ΔI and $\Delta I^{//}$ is not real and comes from the fact that $\Delta I^{//}(\mu_0)$ refers to an intensity emerging slightly off the direction given by μ_0 because of the distortion of the surface. To correct from this effect we should use Eq. (34) instead of (33) to compare emerging intensity at μ_0 in the plane-parallel approximation with emerging intensity of the general spherical case as given by Eqs. (13) and (25). It is useful to note that firstly Eq. (34) is not valid for stars with extended atmosphere and secondly for others stars Eq. (34) is meaningful not too close to the limb where sphericity of the emitting layers is not negligible.

In this section we have derived the analytical perturbation of emerging intensity in three different manners. The first one given by Eq. (13) is derived using an Eulerian formulation. The second one given by Eq. (25) is derived using a Lagrangian formulation. The last one given by Eq. (34) is obtained in the plane-parallel approximation. We have shown that in this last case the perturbation of emerging intensity reduces to what Toutain & Gouttebroze (1993) found but with one restriction: to neglect the h-dependence of ξ_r/r.

Before going to numerical comparisons of the different formulations, we derive expressions for the corresponding flux perturbations.

3. Total flux perturbation

3.1. Spherical case

To obtain the perturbation of total flux ΔF we integrate the perturbation of emerging intensity, given by Eqs. (13) or (25), over the visible disc ($0\leq\phi_0\leq 2\pi$, $\mu_{\rm limb}\leq\mu_0\leq 1$).

$$\Delta F(\mu_{\rm limb}) = \int_0^{2\pi}\int_{\mu_{\rm limb}}^1 \Delta I(\mu_0,\phi_0)\,\mathrm{d}\Sigma_0 \tag{35}$$

where $\mathrm{d}\Sigma_0 = \mu_0\mathrm{d}\mu_0\mathrm{d}\phi_0$ is the projected surface element, taking the radius as unity. In principle we should add an extra-term coming from the deformation of the limb itself but neglect it because the intensity vanishes on the very limb. ΔI is a function of $Y_{lm}(\theta_0^*, \phi_0^*)$ which has first to be transformed according to:

$$Y_{lm}(\theta_0^*,\phi_0^*) = \sum_{p=-l}^{l} c_{mp}^l Y_{lp}(\theta_0,\phi_0) \tag{36}$$

before integrating in ϕ_0 Eq. (35). We easily see that only the component p = 0 contributes to the integral. Consequently Eq. (35) becomes

$$\Delta F(\mu_{\rm limb}) = Y_{lm}(\theta_{obs}^*,\phi_{obs}^*)\int_{\mu_{\rm limb}}^1 \Delta I(\mu_0)\mu_0\mathrm{d}\mu_0 \tag{37}$$

where (θ_{obs}^*,ϕ_{obs}^*) are the angles defining the direction of the observer in the main frame of the Sun. ΔI is now only a function of μ_0 through P_l the Legendre polynomial of degree l. To avoid heavy notation we keep the same notation for a function of (ϕ_0, μ_0) and its integral over ϕ_0.

As in the previous section, it is also interesting to study the plane-parallel case.

3.2. The plane-parallel approximation

Inserting Eq. (34) into Eq. (35) and applying the same method as for the spherical case we find:

$$\begin{aligned}\Delta F(\mu_{limb}) \;=\; &\left[\int_{\mu_{\rm limb}}^1 \delta I^{//}(\mu_0)\mu_0\mathrm{d}\mu_0\right.\\ &\left.+\int_{\mu_{\rm limb}}^1 I^g(\mu_0)\mu_0\mathrm{d}\mu_0\right]Y_{lm}(\theta_{obs}^*,\phi_{obs}^*)\end{aligned} \tag{38}$$

Following Toutain & Gouttebroze (1993) we know that in the plane-parallel approximation the flux perturbation writes:

$$\Delta F^{//}(\mu_{\rm limb}) = Y_{lm}(\theta^*_{obs},\phi^*_{obs})\left[\int_{\mu_{\rm limb}}^1 \delta I^{//}(\mu_0)\mu_0 {\rm d}\mu_0 + \frac{\xi_r}{r}\int_{\mu_{\rm limb}}^1 (\mu_0^2-1)\frac{dP_l(\mu_0)}{d\mu_0}\frac{dI^{//}}{d\mu_0}\mu_0{\rm d}\mu_0 + \frac{\xi_r}{r}\int_{\mu_{\rm limb}}^1\left[\frac{(\mu_0^2-1)}{\mu_0}\frac{dP_l(\mu_0)}{d\mu_0}+2P_l(\mu_0)\right] I^{//}(\mu_0)\mu_0{\rm d}\mu_0\right] \quad (39)$$

where the second and the third integrals take into account the perturbation of the local normal and the distortion of the surface, respectively. These terms are the so-called geometrical terms. A straight comparison between this equation and Eq. (38) shows that the integral of I^g should contain the geometrical effects. Integrating Eq. (32) over ϕ_0 we obtain

$$F^g(\mu_{\rm limb}) = Y_{lm}(\theta^*_{obs},\phi^*_{obs})\int_{\mu_{\rm limb}}^1 I^g(\mu_0)\mu_0{\rm d}\mu_0 = F^{g_1}(\mu_{\rm limb}) + F^{g_2}(\mu_{\rm limb}) \quad (40)$$

with

$$F^{g_1}(\mu_{\rm limb}) = \frac{\xi_r}{r}Y_{lm}(\theta^*_{obs},\phi^*_{obs})\int_{\mu_{\rm limb}}^1 (\mu_0^2-1)\frac{dP_l(\mu_0)}{d\mu_0}\frac{dI^{//}(\mu_0)}{d\mu_0}\mu_0\,{\rm d}\mu_0 \quad (41)$$

and

$$F^{g_2}(\mu_{\rm limb}) = \frac{\xi_r}{r}Y_{lm}(\theta^*_{obs},\phi^*_{obs})\int_{\mu_{\rm limb}}^1 (1-\mu_0^2)P_l(\mu_0)\frac{dI^{//}(\mu_0)}{d\mu_0}{\rm d}\mu_0 \quad (42)$$

F^{g_1} is the contribution of local normal change to the flux perturbation (second term of Eq. 39). To get F^{g_2} in a known form we first have to perform an integration by part. Then

$$F^{g_2} = \frac{\xi_r}{r}Y_{lm}(\theta^*_{obs},\phi^*_{obs})\int_{\mu_{\rm limb}}^1\left[\frac{(\mu_0^2-1)}{\mu_0}\frac{dP_l(\mu_0)}{d\mu_0} + 2P_l(\mu_0)\right] I^{//}(\mu_0)\mu_0{\rm d}\mu_0 - F^{\rm limb} \quad (43)$$

where

$$F^{\rm limb}(\mu_{\rm limb}) = \frac{\xi_r}{r}P_l(\mu_{\rm limb})(1-\mu^2_{\rm limb}) \times I^{//}(\mu_{\rm limb})Y_{lm}(\theta^*_{obs},\phi^*_{obs}) \quad (44)$$

The first term in F^{g_2} is the flux perturbation due to the solar surface distortion (third term of Eq. 39). Therefore we have:

$$\Delta F(\mu_{\rm limb}) = \Delta F^{//}(\mu_{\rm limb}) - F^{\rm limb}(\mu_{\rm limb}) \quad (45)$$

The second term $F^{\rm limb}$ is a term due to limb deformation which was neglected in Eq. (35) because the intensity is supposed to vanish on the limb. But for the plane-parallel approximation the intensity does not vanish on the limb and the limb deformation can not be neglected. Adding this term to Eq. (45) shows that in the plane-parallel approximation, the formula for flux perturbation is the same as the one derived by Toutain & Gouttebroze (1993): i.e. Eq. (39).

In this section we have shown that, in the plane-parallel approximation and if ξ_r/r is not a function of depth, the flux perturbation of the general spherical case reduces to the expression given by Eq. (39) with its corresponding geometrical terms.

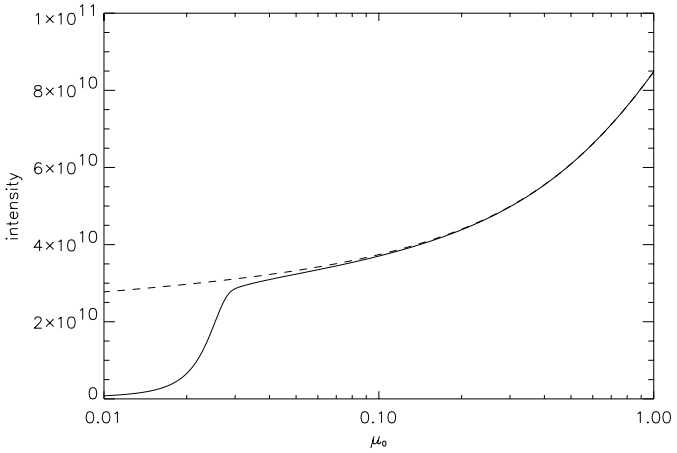

Fig. 3. Intensity for a grey atmosphere as a function of μ_0 in the spherical case (solid line) and the plane-parallel case (dashed line)

4. Numerical comparison of the different approaches

The goal of this section is to compare, from a numerical point of view, the three formulations: Eulerian, Lagrangian and plane-parallel. We use a standard solar model obtained with the code CESAM of the Nice Observatory, (Morel 1997). For simplicity, the eigenfunctions are computed in the adiabatic approximation and to be compatible with the solar model, the radiative transfer is limited to the grey case.

4.1. Intensity at equilibrium

Using Eqs. (1) and (28) with a $\sigma{\rm T}^4$ source function, we first compute the intensity over the disc in the general spherical case and in the plane-parallel case. These intensities are plotted in Fig. 3

As expected the intensity decreases to 0 towards the limb in the spherical case, due to rarefaction of the atmosphere, and tends to the source function at the temperature of the first layer of the model in the plane-parallel case. For $\mu_0 \leq 0.1$ the total optical thickness at visible wavelengths along the line of sight becomes smaller than 1 and the plane-parallel approximation assuming an infinite extended atmosphere is no longer appropriate to describe the problem.

In order to compare the theoretical behavior of the intensity at the limb to the observations we have considered various papers on limb darkening. In most of them, the authors try to fit observations of intensity on the disk with polynomials, discard-

ing the first 7″ of the limb, which is the region we are interested in. Nevertheless, Dunn (1959) has measured the intensity of the continuum at the very limb of the solar disk and he shows that the intensity drops off very rapidly on a distance scale smaller than 1″, a result which is well reproduced by our model and confirmed by Pierce & Slaughter (1977).

4.2. Intensity perturbation

We compute now the perturbations of emerging intensity using Eqs. (13), (25) and (34) for the Eulerian, Lagrangian and plane-parallel description, respectively. For a given mode (n, l, m) we write

$$\Delta I_\nu^{nlm}(\mu_0,\phi_0) = \Delta I_\nu^{nlm}(\mu_0)\cos(\omega t + m\phi_0) \qquad (46)$$

assuming the rotation axis of the Sun is pointing towards the observer (Z-axis). Usually, observations are made in or close to the ecliptic plane which corresponds to a rotation axis aligned to the Y-axis instead of the Z-axis. In this case, using Eqs. (36) and (46), the observed intensity perturbations can be written as linear combinations of the previous perturbations

$$\Delta I_\nu^{nlm}(\mu_0,\phi_0) = \sum_{p=-l}^{l} c_{mp}^{l}\Delta I_\nu^{nlp}(\mu_0)\cos(\omega t + p\phi_0) \qquad (47)$$

where $\Delta I_\nu^{nlp}(\mu_0)$ refer to the intensity perturbation for a rotation axis pointing towards the observer and the c_{mp}^{l} are the rotation matrix elements.

We focus here on low-degree p and g modes for a rotation axis pointing towards the observer. According to Kumar et al.(1996), the very low-radial order g modes are expected to have the highest surface velocity amplitudes (few tenths of mm/s). We therefore only look at the intensity perturbation induced by low-order g modes but also p modes assuming a surface velocity of 1 mm/s.

The $\Delta I_\nu^{nlp}(\mu_0)$ normalized with intensity are plotted in Figs. 4,5,6 for p modes l=0,1 and 2 of order n=3, respectively, and in Figs. 7,8 for l=1,2 n=3 g modes as a function of μ_0. Solid lines are both for intensity perturbation using Eulerian and Lagrangian formulations, whereas dashed line is for intensity perturbation obtained in the plane-parallel case. Note that, as explained in Sect. 2.2, in the case of the Sun and for visible continuum observations below μ_0=0.03 the Lagrangian description is meaningless and the corresponding intensity perturbation therefore not computed. In each case the three curves overlap perfectly up to 0.1, the solar photosphere being very thin the plane-parallel case is still a good approximation there. Below 0.1 the effect of sphericity takes place and for modes with $l+m$ even the two solid curves exhibit a strong change (notice the log-scale) in the emerging intensity perturbation whereas the dashed curve keeps its monotonic shape. As explained in the previous subsection, below 0.1 the Sun becomes more and more transparent increasing the contribution of the other hemisphere. This effect is significant and of the order of several ppms, only for modes having non vanishing eigenfunctions at the limb, that is to say mode with (l+m) even.

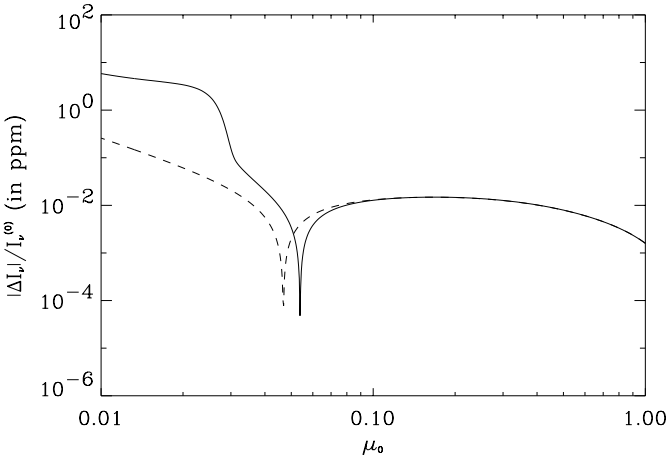

Fig. 4. Modulus of relative intensity perturbation due to a 1 mm/s - l=0 n=3 p mode as a function of μ_0: in the spherical case (solid line, curves for Eulerian and Lagrangian formulations are identical) and the plane-parallel case (dashed line).

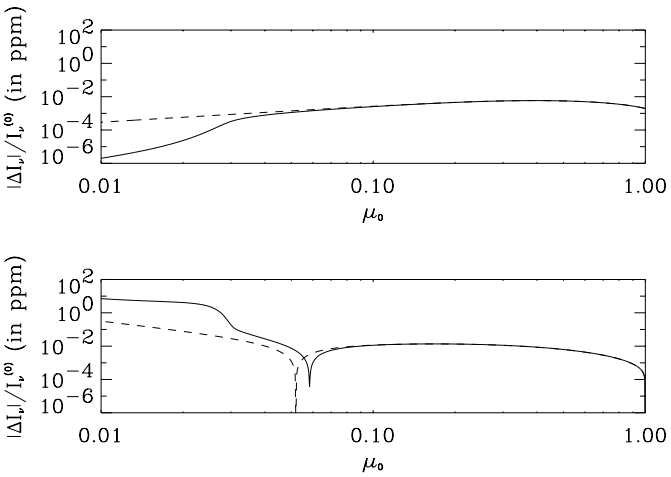

Fig. 5. Modulus of relative intensity perturbation due to a 1 mm/s - l=1 n=3 p mode for m=0 (*top panel*) and m=1 (*bottom panel*) as a function of μ_0 in the spherical case (solid line, curves for Eulerian and Lagrangian formulations are identical) and the plane-parallel case (dashed line).

From these computations, we conclude that a strong signature of some of the low-degree p and g modes is expected on the very limb of the solar disc. Appourchaux & Toutain (1998) claim they have detected low-degree p modes in the guiding pixel signals ($0 \leq \mu_0 \leq 0.05$) of the LOI/VIRGO instrument with amplitudes 3 times larger as those of the p modes in full-disk. Toner & Jefferies (1998) have also found some evidence of enhancement of p-mode amplitude in MDI intensity data at the solar limb. Hill & Caudell (1979) have noticed changes of the apparent limb darkening function in solar radius data.

4.3. Flux perturbation

In this section, we test the numerical accuracy and the agreement between Eulerian, Lagrangian and plane-parallel formulations

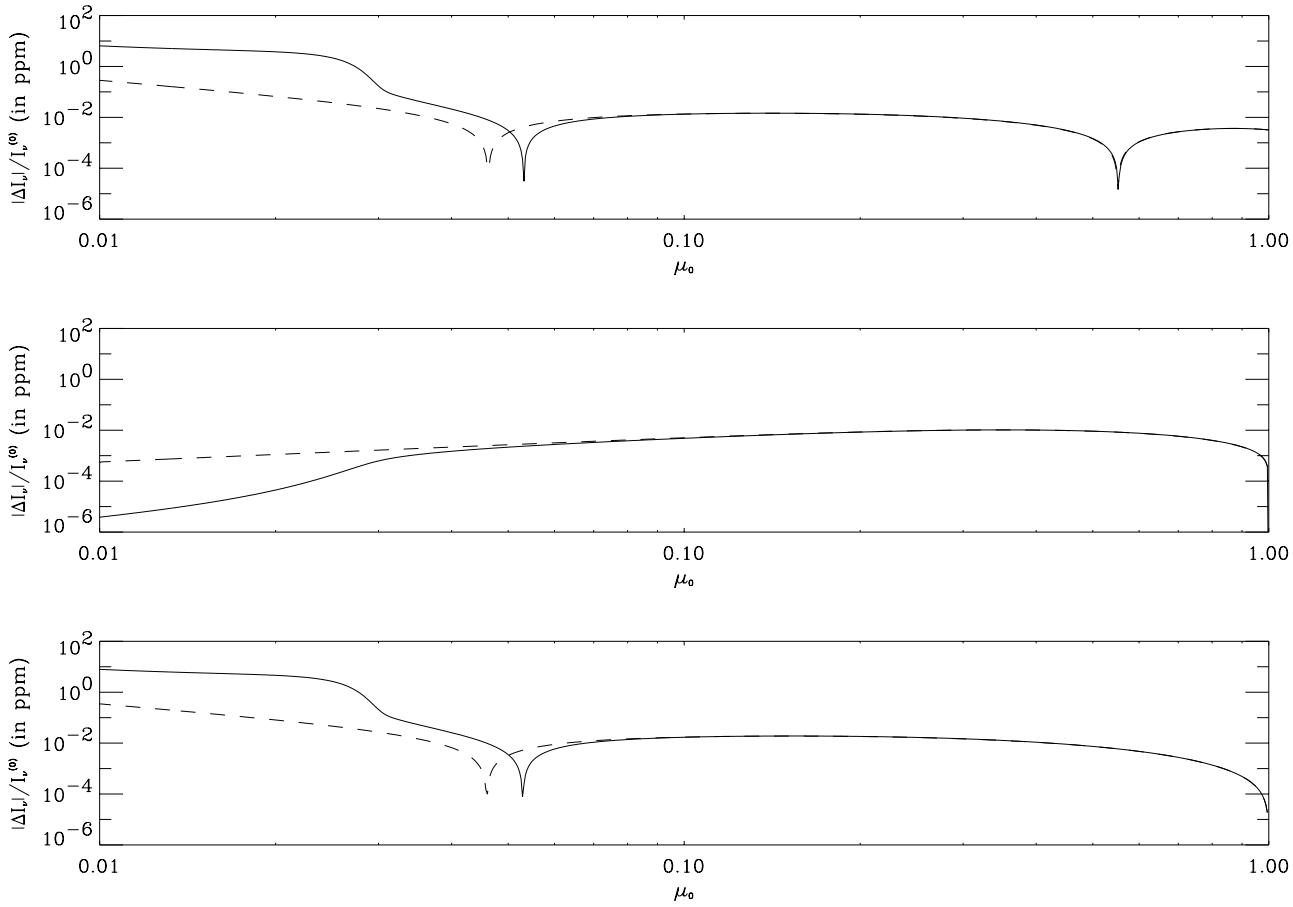

Fig. 6. Modulus of relative intensity perturbation due to a 1 mm/s - l=2 n=3 p-mode for m=0,1 and 2 (*top* to *bottom*) as a function of μ_0 in the spherical case (solid line, curves for Eulerian and Lagrangian formulations are identical) and the plane-parallel case (dashed line).

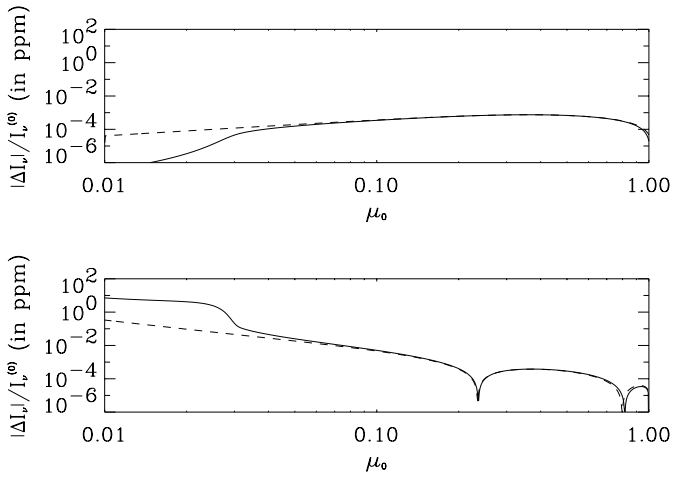

Fig. 7. Perturbation of intensity due to a 1 mm/s - l=1 n=3 g-mode for m=0 (*top panel*) and m=1 (*bottom panel*) as a function of μ_0 in the spherical case (solid line, curves for Eulerian and Lagrangian formulations are identical) and the plane-parallel case (dashed line).

using various numbers of mesh points for integration in z and μ_0. According to the computations carried out in the previous section intensity perturbations derived with each formulation agree very well on most of the disk. Nevertheless differences are quite large at the limb and it is therefore interesting to check by how much theses differences can modify the corresponding flux perturbations. In Table 1 are reported the flux perturbations due to l=1,2 n=3 g and p modes as a function of the methods we used and the grid mesh for integration. The methods are Eulerian, Lagrangian formulations with Eq. (37) and plane-parallel approximation with Eq. (39), respectively. Flux perturbations for each degree are normalized to the value given by the Eulerian formulation and the finest grid mesh which is supposed to give the best value. We have selected for the integration in z (or h) an upper boundary at τ=20 and a grid mesh between $100 \leq N_z \leq 12500$ points and for integration in μ_0 a grid mesh between $25 \leq N_\mu \leq 800$ points regularly spaced in Log(μ_0). $\mu_{\rm limb}$ is taken as 0.001. Because the Lagrangian description does not permit to go below μ_0=0.03, we have replaced its value below 0.03 with the value given by the Eulerian description. Moreover, though the plane-parallel approximation is meaningless below 0.1 we have performed the integration up to 0.001 to test the accuracy of this method as far as flux perturbation is concerned. As we can see from the tables, all the descriptions give values converging towards a same flux perturbation with a precision of a percent. We note that the slowest convergence is obtained with the Eulerian description which requests a very fine grid to accu-

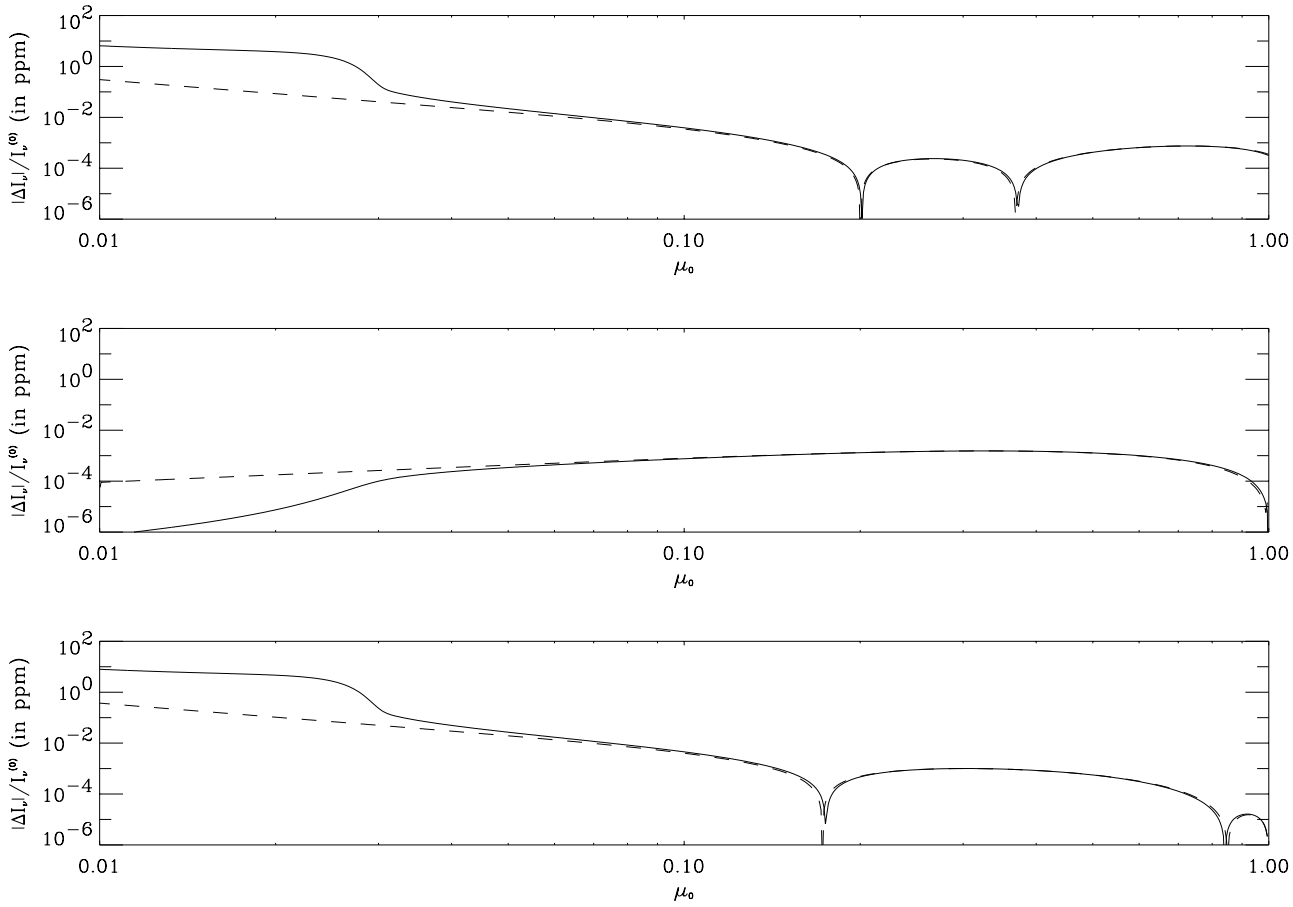

Fig. 8. Perturbation of intensity due to a 1 mm/s - l=2 n=3 g-mode for m=0,1 and 2 (*top* to *bottom*) as a function of μ_0 in the spherical case (solid line, curves for Eulerian and Lagrangian formulations are identical) and the plane-parallel case (dashed line).

rately cancel the advection terms. Instead of using the Eulerian description for numerical purpose, it is therefore better to use the Lagrangian description which leads to a faster convergence. It is interesting to note that though the plane-parallel approximation does not describe correctly the intensity perturbation near the limb it leads, for the given modes, to a flux perturbation in good agreement with the exact perturbation obtained in the general spherical case. Fig. 9 shows in percent the relative difference between Eulerian and plane-parallel flux perturbations as a function of mode frequency for l=1,2 modes. The effect due to sphericity of the emitting layers is therefore visible only for high frequencies. For l=1 modes the agreement is good whatever the frequency is, because the radial displacement function vanishes on the limb. Sphericity effects are therefore negligible for g-mode flux perturbations and the previous computations done assuming a plane-parallel atmosphere are still valid (Toutain et al. 1995).

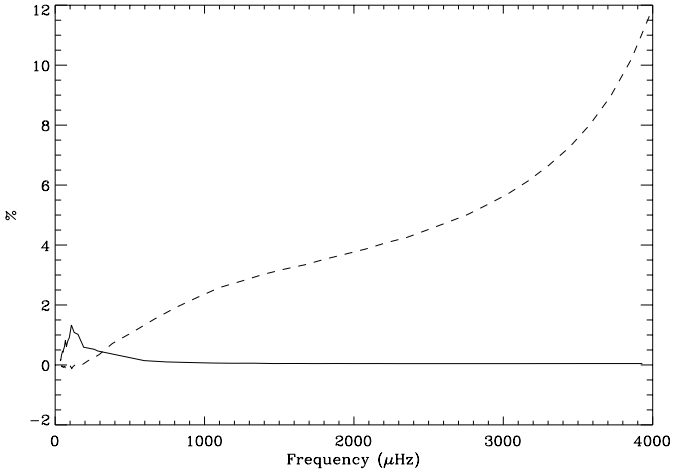

Fig. 9. Relative difference in percent of the flux perturbations using Eulerian formalism and plane-parallel approximation as a function of mode frequency (solid line is for l=1 and dashed line for l=2).

5. Conclusions

We have derived analytical expressions for intensity and flux perturbations in the general spherical case using both Eulerian and Lagrangian descriptions and have shown their equivalence. Nevertheless, the Lagrangian description is more suited for numerical purposes than the Eulerian one, because this last one requests to deal with cancellation of advection terms which makes computations accurate only with a high number of mesh grid points.

Table 1. Normalized flux perturbation as a function of N_z the grid mesh in z and N_μ the grid mesh in μ. For a given (N_z,N_μ), columns from left to right are for Eulerian (E), Lagrangian (L) and plane-parallel (//) methods, respectively whereas rows from top to bottom are for g-modes l=1,2 n=3 (G_{31} and G_{32}) and p-modes l=1,2 n=3 (G_{31} and G_{32}), respectively.

N_μ; N_z	100			500			2500			12500			
	E	L	//	E	L	//	E	L	//	E	L	//	
25	137.2	1.03	1.00	5.69	0.98	0.96	1.17	0.98	0.95	0.99	0.98	0.95	G_{31}
	14.6	1.03	1.02	1.46	0.99	0.99	1.01	0.99	0.99	0.99	0.99	0.99	G_{32}
	53.4	0.75	1.01	2.47	0.73	1.00	0.80	0.73	1.00	0.73	0.73	1.00	P_{31}
	36.3	0.85	1.05	1.95	0.78	0.98	0.82	0.77	0.97	0.78	0.77	0.97	P_{32}
50	125.2	1.04	1.03	5.65	0.99	0.99	1.18	0.99	0.98	1.00	0.99	0.98	G_{31}
	13.4	1.03	1.03	1.46	1.00	1.00	1.02	1.00	1.00	1.00	1.00	1.00	G_{32}
	47.8	1.16	1.02	2.82	1.15	1.01	1.21	1.15	1.01	1.15	1.15	1.01	P_{31}
	32.6	1.17	1.08	2.23	1.10	1.02	1.14	1.09	1.01	1.10	1.10	1.01	P_{32}
100	115.7	1.05	1.03	5.65	0.99	0.99	1.18	0.99	0.99	1.00	0.99	0.99	G_{31}
	12.5	1.04	1.03	1.46	1.00	1.00	1.02	1.00	1.00	1.00	1.00	1.00	G_{32}
	42.4	0.87	1.02	2.51	0.85	1.01	0.92	0.85	1.00	0.85	0.85	1.00	P_{31}
	28.9	0.98	1.08	2.02	0.90	1.02	0.94	0.90	1.02	0.90	0.90	1.02	P_{32}
200	117.0	1.05	1.04	5.65	0.99	0.99	1.18	0.99	0.99	1.00	0.99	0.99	G_{31}
	12.6	1.04	1.03	1.46	1.00	1.00	1.02	1.00	1.00	1.00	1.00	1.00	G_{32}
	43.1	1.06	1.02	2.70	1.04	1.00	1.10	1.04	1.00	1.04	1.04	1.00	P_{31}
	29.4	1.10	1.08	2.15	1.03	1.02	1.07	1.02	1.02	1.03	1.02	1.02	P_{32}
400	114.6	1.05	1.04	5.70	0.99	0.99	1.18	0.99	0.99	1.00	0.99	0.99	G_{31}
	12.4	1.04	1.03	1.47	1.00	1.00	1.02	1.00	1.00	1.00	1.00	1.00	G_{32}
	41.8	1.01	1.02	2.68	0.99	1.00	1.06	0.99	1.00	1.00	0.99	1.00	P_{31}
	28.6	1.08	1.08	2.13	1.00	1.02	1.04	0.99	1.02	1.00	0.99	1.02	P_{32}
800	114.5	1.05	1.03	5.70	0.99	0.99	1.18	0.99	0.99	1.00	0.99	0.99	G_{31}
	12.3	1.04	1.03	1.47	1.00	1.00	1.02	1.00	1.00	1.00	1.00	1.00	G_{32}
	41.6	1.02	1.02	2.68	1.00	1.00	1.07	1.00	1.00	1.00	1.00	1.00	P_{31}
	28.4	1.08	1.08	2.14	1.00	1.02	1.04	1.00	1.02	1.00	1.00	1.02	P_{32}

In the limit of a plane-parallel atmosphere we have shown that the analytical expressions for intensity and flux perturbations reduce to the formulas given by Toutain & Gouttebroze (1993) including the so-called geometrical effects. We have established that the plane-parallel approximation leads generally, for solar g modes and low-frequency p modes, to intensity and flux perturbations in good agreement with those obtained in the general spherical case. Nevertheless on the very limb the solar atmosphere becomes transparent and spherical case computations show that both some p and g modes are expected to produce very large intensity perturbations though too small to significantly affect the flux perturbations. This effect unexpected with plane-parallel calculations is a consequence of the sphericity of the emitting layers. It could explain some observational evidences of the existence of solar oscillations on the solar limb with larger amplitudes than expected (Appourchaux & Toutain 1998; Toner & Jefferies 1998). However nonadiabatic computations including the oscillation-convection interaction are needed to make reliable comparisons with observations.

Acknowledgements. The authors would like to thank P. Gouttebroze and W.A. Dziembowski for useful comments. T. Toutain would also like to thank the Institute of Theoretical Astrophysics of Oslo for its support.

References

Andersen B.N., 1996, A&A 312, 610
Appourchaux T., Toutain T., 1998, Symposium IAU 181, poster volume, 5
Buta R.J., Smith M.A., 1979, ApJ 232, 213
Balmforth N.J., 1992, MNRAS 255, 603
Berthomieu G., Provost J., 1990, A&A 227, 563
Chandrasekhar S., 1960, Radiative transfer. Dover Publications
Dunn R.B., 1959, ApJ 130, 972
Dziembowski W., 1977, Acta Astron. 27, 203
Gonczi G., Osaki Y., 1980, A&A 84, 304
Gough D.O., 1977, ApJ 214, 196
Gouttebroze P., Toutain T., 1994, A&A 287, 535
Hill H.A., Caudell T.P., 1979, MNRAS 186, 327
Kumar P., Quataert E.J., Bahcall J.N., 1996, ApJ 458, L83
Morel P., 1997, A&AS 124, 597
Pierce A.K., Slaughter C., 1977, Sol. Phys. 51, 25
Staude J., Dzhalilov N.S., Zhugzhda Y.D., 1994, Sol. Phys. 152, 227
Toner C G., Jefferies, S. M. 1998, to appear in: Structure and Dynamics of the Interior of the Sun and Sun-like Stars. SOHO6/GONG98 workshop, ESA proceedings
Toutain T., Gouttebroze P., 1993, A&A 268, 309
Toutain T., Berthomieu G., Provost J., Gouttebroze P., 1995, Proceedings of the IV SOHO Workshop, ESA SP-376, 419